Molecular structure and dynamics of C-1-adamantyl substitutedN-unsubstituted pyrazoles studied by solid state NMRspectroscopy and X-ray crystallography

ARTICLE *in* JOURNAL OF THE CHEMICAL SOCIETY PERKIN TRANSACTIONS 2 · SEPTEMBER 1997

DOI: 10.1039/A607436G

Molecular structure and dynamics of *C*-1-adamantyl substituted *N*-unsubstituted pyrazoles studied by solid state NMR spectroscopy and X-ray crystallography

Rosa María Claramunt,[a] María Dolores Santa María,[a] Isabelle Forfar,[a] Francisco Aguilar-Parrilla,†,[b] María Minguet-Bonvehí,[b] Oliver Klein,[b] Hans-Heinrich Limbach,[b] Concepción Foces-Foces,[c] Antonio L. Llamas-Saiz[c] and José Elguero[d]

[a] *Departamento de Química Orgánica y Biología, Facultad de Ciencias, UNED, Senda del Rey s/n, 28040 Madrid, Spain*
[b] *Institut für Organische Chemie, Freie Universität Berlin, Takustrasse 3, 14195 Berlin, Germany*
[c] *Departamento de Cristalografía, Instituto de Química Física 'Rocasolano', CSIC, Serrano, 119, E-28006 Madrid, Spain*
[d] *Instituto de Química Médica, CSIC, Juan de la Cierva 3, 28006 Madrid, Spain*

The influence of the 1-adamantyl group on the structure and the proton transfer dynamics of *N*-unsubstituted pyrazoles has been determined. Four compounds have been labelled with ^{15}N and studied by variable temperature ^{15}N CP MAS NMR spectroscopy: 3(5)-(1-adamantyl)pyrazole 2, 4-(1-adamantyl)pyrazole 3, 3,5-dimethyl-4-(1-adamantyl)pyrazole 4 and 3,5-di(1-adamantyl)pyrazole 5. Compound 2 (a 1:1 mixture of both tautomers) is a long chain of hydrogen bonded molecules ('catemer') and as in most catemers there is no proton transfer since it would imply an 'infinite' number of proton jumps. Compound 3, although also a 'catemer', is possibly an exception to this rule, in that it seems to show proton transfer. In the solid state, compounds 4 and 5 should be cyclic hydrogen-bonded structures, dimers or trimers, but the activation energies for proton transfer, about 39 kJ mol^{-1}, are quite low compared with those of 3,5-dimethylpyrazole. It appears that the quasi-spherical shape of the 1-adamantyl substituent and its solid-state plasticity may play a role in lowering these barriers. The crystal structure of 2 has been determined by X-ray analysis. Individual molecules of 2 form chains through N–H · · · N hydrogen bonds ('catemers') very similar to those already described for 4-(1-adamantyl)-pyrazole and for pyrazole itself; however, the packing of these catemers is different. Tautomers 2a and 2b are present in the crystal in a 1:1 ratio, forming alternating chains of hydrogen-bonded molecules (2a · · · 2b · · · 2a · · · 2b · · ·); the NH hydrogen atoms are linked to both nitrogen positions (N1 and N2) and show a 1:1 disorder.

Introduction

The substitution of the hydrogen atoms at positions C3, C4 and C5 of an *N*-unsubstituted (*N*H)-pyrazole affects the spatial ordering of the molecules in such a way that different intermolecular hydrogen-bonded complexes are formed in the solid state depending on the nature of the substituents.[1–6] This is the case for several pyrazole derivatives, previously studied by X-ray crystallography, where different classes of hydrogen-bonded networks, such as dimers, trimers, tetramers or longer chains ('catemers') are found in the crystal.[1–6] In addition, double, triple and even quadruple intermolecular proton transfer processes were detected in the cyclic hydrogen bonded complexes by ^{13}C CP MAS NMR spectroscopy (CP: cross polarization, MAS: magic angle spinning).[1] After labelling the compounds with ^{15}N, equilibrium constants, rate constants and additional information about the proton tautomerism were obtained by variable temperature (VT) ^{15}N CP MAS NMR spectroscopy.[2–6] Since then, we have used pyrazoles as model compounds in order to study how the mechanism of proton exchange depends on the number of protons transferred.[7–9]

Further investigations showed that substituents which can adopt different conformations[10] with respect to the pyrazole ring affect the equilibrium and rate constants of the proton tautomerism.[5] This is the case for 3,5-di-*tert*-butylpyrazole **1** where the *tert*-butyl group conformation, different at C3 and C5, strongly affects the degeneracy of the intradimer proton tautomerism. As a consequence, an asymmetric exchange system is observed by CP MAS NMR, *i.e.* one tautomer is preferentially formed in the solid state although the pyrazole ring is symmetrically substituted ($R^3 = R^5$). By combination of X-ray crystallography and ^{15}N CP MAS NMR spectroscopy the complex exchange process in **1** has been fully characterized.[5]

In the present work, we were interested in studying the influence of the 1-adamantyl group on the structure and

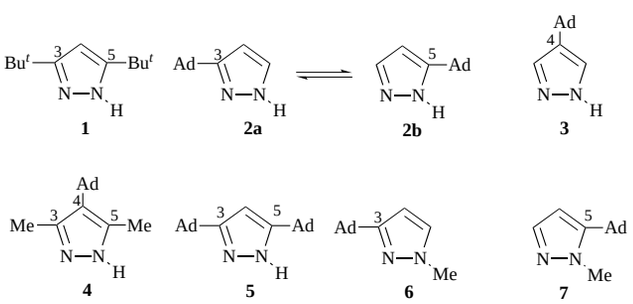

Pyrazole derivatives studied

† Present address: Schering AG, QS-QE2, 13353 Berlin, Germany.

Table 1 ^{13}C and ^{15}N chemical shifts (in ppm) of adamantyl substituted pyrazoles in the solid state at room temperature (300 K) unless otherwise indicated.[a] For comparison the values for pyrazole and 3,5-dimethylpyrazole are also included.[14]

Compound	C3	C4	C5	N–H	=N–
Pyrazole pz[b]	139	107	128	170	248
3-(1-Adamantyl)pz **2a**[c]	161.1	99.6	128.3	163.5	240.4
5-(1-Adamantyl)pz **2b**[c]	138.1	99.6	152.3	165.8	245.0
4-(1-Adamantyl)pz **3** [d,i]	134.5	132.8	123.7	166.5	242.7 251.7
3,5-Dimethylpz[b,j]	146	105	141	167	241
3,5-Dimethyl-4-(1-adamantyl)pz **4**[e]	144.5br	121.2	134.3br	166.6[k]	240.5[k]
3,5-Di(1-adamantyl)pz **5**[f]	152–160br	93.7	152–160br	159.6[l]	241.0[l]
1-Methyl-3-(1-adamantyl)pz **6**[g]	162.1	102.5	130.2	156.2	262.8
1-Methyl-5-(1-adamantyl)pz **7**[h]	138.6	103.5	150.3 151.4	160.0	274.8

[a] All ^{15}N chemical shifts relate to external solid $^{15}NH_4Cl$ and are given with an error of ±0.3 ppm. ^{13}C chemical shifts are given with respect to $SiMe_4$. [b] Ref. 14. Adamantyl carbon chemical shifts: [c] Cα 33.0 and 34.0, Cβ 42.6, Cγ 28.7, Cδ 36.6 ppm; [d] Cα 31.4, Cβ 44.8, Cγ 29.3, Cδ 37.0 ppm; [e] Cα, 32.0, Cβ 42.3, Cγ 29.4, Cδ 36.5 ppm; [f] Cα 33.6, Cβ 43.4, Cγ 28.6 and 29.3, Cδ 37.2 ppm; [g] Cα 34.2, Cβ 42.9, Cγ 29.1, Cδ and CH_3 37.1 ppm; [h] Cα 33.3, Cβ 40.9, Cγ 29.1, Cδ and CH_3 37.6 ppm. [i] Ref. 13. [j] T = 260 K. [k] T = 230 K. [l] T = 252 K.

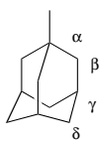

dynamics of pyrazoles, since here, as in the case of the *tert*-butyl substituent,[5] dynamic conformational disorder is expected. Two reasons prompted us to investigate this class of pyrazole derivatives in the solid state: (*i*) the crystal plasticity (easy molecular motion about mean positions in the lattice) of adamantane itself which usually results in special physical properties of its derivatives[11,12] and, (*ii*) as already stated, the possibility of finding dynamic conformational disorder of the adamantyl substituent around the adamantyl–pyrazole $C(sp^3)$–$C(sp^2)$ bond, *i.e.* two or more conformations, which could affect the crystal structure and proton transfer dynamics as in the case of **1**.[5]

Four symmetric and asymmetric 1-adamantyl-substituted NH-pyrazoles (**2**–**4**) and two 1-adamantyl-substituted *N*-methylpyrazoles (**6**, **7**) were synthesized. For the 3(5)-(1-adamantyl)-pyrazole **2** a non-degenerate system should be expected in the solid state which could result in the presence of only one tautomer. However, the results obtained by ^{13}C and ^{15}N CP MAS NMR spectroscopy show that tautomers **2a** and **2b** are present in equal amounts in the crystal. In the case of the three other compounds, although symmetrically substituted, the orientation of the adamantyl group affects the symmetry of the crystal resulting in different equilibrium constants for the tautomerism.

Results and discussion

For the following discussion a summary of the crystallographic results concerning adamantyl-*N*H-pyrazoles **2**–**5** is necessary. We failed to obtain crystals of 3,5-diadamantylpyrazole **5**; in the case of 3,5-dimethyl-4-adamantylpyrazole **4**, crystals were obtained but they proved to be twinned. The case of compounds **2** and the already published **3**[13] will be discussed in detail in the corresponding sections.

We show here that in the solid state the adamantyl group orientation and proton tautomerism are completely different in the four pyrazole derivatives studied. Therefore, we prefer to present and discuss the crystallographic data (when available) and NMR spectroscopic results for each compound separately.

3(5)-(1-Adamantyl)pyrazole 2

The ^{13}C and ^{15}N CP MAS NMR spectra of **2** obtained at room temperature (300 K) are shown in Fig. 1. All ^{13}C and ^{15}N chemical shifts are reported in Table 1. In the ^{13}C NMR spectrum [Fig. 1(*a*)] two signals are observed for both the C3 and the C5 atoms of the pyrazole ring, indicating that the two tautomers,

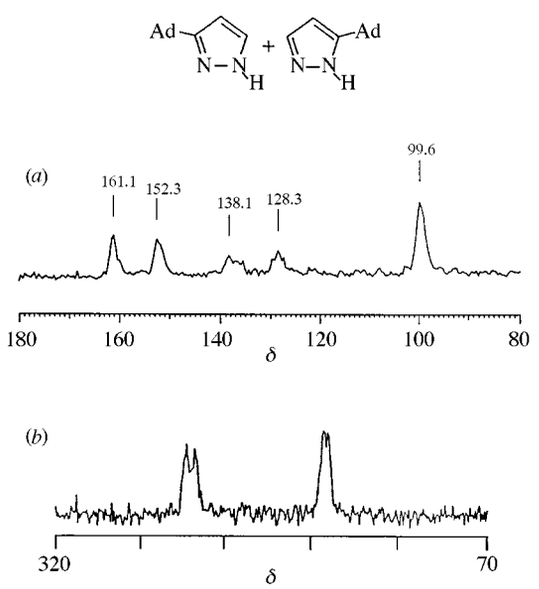

Fig. 1 (*a*) 50.32 MHz ^{13}C CP MAS NMR spectrum of **2** recorded at room temperature (300 K): 7 s ^1H-90° pulse width, 4 ms contact pulse, 5 s repetition time, spectral width 20 kHz; (*b*) room temperature (300 K) 9.12 MHz ^{15}N CP MAS NMR spectrum of **2**: 5.5 s ^1H-90°, 5 ms CP-time, 4 s recycle delay, spectral width of 7 kHz, no line broadening used

3-(1-adamantyl)- **2a** and 5-(1-adamantyl)pyrazole **2b** are present in the solid state. Increment calculations based on the effect of the adamantyl group on the ^{13}C chemical shifts of the pyrazole-substituted carbon atom‡[14] lead to the conclusion that the outer C3/C5 signals at 161.1/128.3 ppm must be assigned to the 3-(1-adamantyl) tautomer **2a**, and the inner C3/C5 signals at 138.1/152.3 ppm to the 5-(1-adamantyl) tautomer **2b**. The chemical shift of 99.6 ppm for the C4 atom is the same for the two tautomers, which seem to be present in similar amounts in the crystal.

‡ The ^{13}C chemical shift values obtained for pyrazole are 139 (C3), 107 (C4) and 128 ppm (C5) (see ref. 18). Introducing an adamantyl group at C4 results in a ^{13}C chemical shift of 132.8 ppm for this C atom, *i.e.* an increment of +25.8 ppm (see ref. 14). With this increment we obtain theoretical values for 3-(1-adamantyl)pyrazole **2a** of 165 ppm (C3) and *ca.* 128 ppm (C5), and of *ca.* 139 ppm (C3) and 154 ppm (C5) for 5-(1-adamantyl)pyrazole **2b**, which are in excellent agreement with the experimental values obtained.

Table 2 ^{1}H chemical shifts in ppm, ^{1}H–^{1}H and ^{1}H–^{15}N coupling constants (J/Hz) of 3(5)-(1-adamantyl)pyrazole **2**, 1-methyl-3-(1-adamantyl)pyrazole **6** and 1-methyl-5-(1-adamantyl)pyrazole **7** in $CDCl_3$

Compd.	δ(H3)	δ(H5)	δ(H4)	^3J[H3(5)–H4]	^2J(H3–N2)	^3J(H3–N1)	^2J(H5–N1)	^3J(H5–N2)	^3J(H4–N1)	^3J(H4–N2)
2 (exp.)	7.49	7.49	6.09	2.05	9.9	5.3	9.9	5.3	3.4	3.4
2 (calc.)[a]	—	—	—	2.03	9.8[b]	5.3	9.8	5.3	2.8[c]	4.0[c]
6	—	7.23	6.05	2.20	—	—	4.5	0.0	6.0	0.9
7	7.33	—	5.98	1.95	12.5	8.0	—	—	1.1	5.6

[a] Assuming 1/3 of tautomer **2a** (using compound **6** as model) and 2/3 of tautomer **2b** (using compound **7** as model). [b] For instance, $\frac{2}{3}$(12.5 Hz) + $\frac{1}{3}$(4.5 Hz) = 9.8 Hz. [c] Average value 3.4 Hz.

The ^{15}N CP MAS NMR spectrum of **2** shown in Fig. 1(*b*) corroborates this finding. The low-field signal corresponding to the non-protonated nitrogen atoms and the high-field one arising from the corresponding protonated nitrogen neighbours are split into doublets, corresponding to the presence of both tautomers in the crystal: **2a** showing signals at 163.5 (N–H) and 240.4 ppm (=N–) and **2b** with signals at 165.8 (N–H) and 245.0 ppm (=N–) (see Table 1).

The assignment of the signals to the different tautomers was carried out by comparison with the ^{15}N chemical shifts obtained for the 1-methyl derivatives (see Table 1). In all cases the =N– signals are much broader than the N–H ones. Since the chemical shift anisotropy of the former is larger, we think that the observed inhomogeneous line broadening is due to the influence of a random distribution of adamantyl group conformations on the chemical shift of the non-protonated nitrogen atoms of both tautomers.[5] This influence is less pronounced in the case of the protonated nitrogen atoms, leading to a difference in the line-width of both signals.[5,15] Both pairs of signals show, however, the same integral, indicating a 1:1 ratio for the two tautomers, *i.e.* an equilibrium constant, $K_{12} = 1$.

In order to detect possible dynamic processes, variable temperature ^{15}N CP MAS NMR experiments were carried out on the ^{15}N-labelled sample. However, in the temperature range explored of 300–375 K (mp 388 K) no sign of adamantyl group rotation, nor of proton transfer was observed. In the first case, the =N– signals of both tautomers should sharpen, indicating an average conformation of the adamantyl group on the NMR timescale.[5] In the second case, a broadening of all lines should then be observed as the temperature is raised.

It is interesting to note that this is the second asymmetric substituted pyrazole derivative where both tautomers have been found to be present in the solid state with an equilibrium constant of $K_{12} = 1$. The first example was the A polymorph of the 3(5)-phenyl-5(3)-methyl derivative where, in addition, a quadruple intermolecular proton transfer was observed.[6]

Since both tautomers **2a** and **2b** were present in a 1:1 ratio in the solid state, we decided to determine the equilibrium constant in solution. We assumed that if they co-crystallize, their difference in energy should be small. The ^{1}H NMR results in $CDCl_3$, necessary to determine the equilibrium constant by interpolation, are reported in Table 2 (for more NMR data, see Experimental section). Using coupling constants, which are quite independent of the solvent, the result of the interpolation shows $\frac{1}{3}$ of tautomer **2a** and $\frac{2}{3}$ of tautomer **2b**; with these populations, the coupling constants are well reproduced (second row of Table 2). The equilibrium constant K_{12} is equal to 0.5 [$\Delta G°$ (at 300 K) = 1.7 kJ mol^{-1}] which justifies our assumption. It remains to be explained why the 5-adamantyl tautomer is the most abundant in solution, a rather unusual result since in most pyrazoles the 3-substituted tautomer is the more stable.[16] Results for other *N*H-pyrazoles suggest that the reason is the extraordinarily high polarizability of the 1-adamantyl substituent ($\sigma_\alpha = -0.95$).[17,18] The ^{15}N chemical shifts in $CDCl_3$ solution (−156.7 and −124.5 ppm, see Experimental) interpolated within those in the solid state (Table 1, corrected by +346.4 ppm) correspond to 30% of tautomer **2a** and 70% of tautomer **2b** (the signal at −156.7 ppm corresponds to the nitrogen atom close to the adamantyl substituent and that at −124.5 ppm to the nitrogen atom far from the adamantyl substituent), percentages close to those obtained from ^{1}H NMR.

X-Ray analysis. Selected geometric characteristics of the molecular structure together with the parameters describing the hydrogen bond interactions are reported in Table 3. The numbering scheme is shown in Fig. 2(*a*) for one of the two crystallographically independent molecules present in the asymmetric unit cell. The pattern of bond distances and angles in the pyrazole moiety is more regular than that of the pyrazole parent compound[19] with respect to the different nature of N(1) and N(2) [–NH– *vs.* –N=]. This is an indication of proton disorder,[20] which was confirmed after the experimental localization of the N–H hydrogen atoms. We found a 1:1 mixture of tautomers **2a** and **2b** in the crystal. Fig. 2(*b*) represents this disorder; the notation **A**/**B** corresponds to the adamantyl conformation (sequence **B**···**B**···**A**···**A**···**B**···**B**) while the tautomers form a chain **2a**···**2b**···**2a**···**2b**···**2a**···**2b** (or the equivalent **2b**···**2a**···**2b**···**2a**···**2b**···**2a**) depending on the position of the first NH proton. However, the internal bond angles at the N atoms of the pyrazole ring are significantly different, due to the influence of the substituent, as has been reported for monosubstituted benzenes.[21] The angular distortions at *ipso*- and *ortho*-positions induced by the 1-adamantyl group in compound **3**[13] compared with pyrazole itself have been calculated (−1.9 and 0.9° respectively). These values have been applied to the equivalent positions of compound **2** (positions 1 and 4 for *ortho*; 5 for *ipso*) in a symmetrized pyrazole molecule and they are in good agreement with the experimental ones in Table 3 (calculated values of 109.2, 105.3 and 107.6° for bond angles at positions 1, 4 and 5, respectively).

With regard to the pyrazole ring, the 1-adamantyl moiety displays the conformation reported in Table 3. The tricyclic structure is formed by four six-membered C rings presenting an almost perfect chair conformation. The ranges for the $q2$ and $\theta2$ Cremer and Pople parameters[22] are 0.002(2)–0.020(2) Å and 0.2(2)–1.8(2)°, respectively; *cf.* $q2 = \theta2 = 0.0$ for a perfect chair.

The secondary structure of compound **2** is very similar to those of the previously described structures of pyrazole[19] and compound **3**,[13] as can be seen in Figs. 2(*b–d*), and in spite of the different symmetry found in the crystals. The 8-shaped hydrogen-bonded chains of the molecules maintain the same pattern of hydrogen bond interactions, Fig. 3. The N–H···N hydrogen bonds are the primary ones and they are similar in all three cases (Table 3). However, the main differences are the changes in the geometry of the weaker C–H···π electron cloud contacts that help to stabilize the cross-linked helix (Table 3). Their strength, as measured by their geometrical parameters, decrease in the following order: compound **2** > pyrazole > compound **3**. The crystal structure of **2** is formed by centrosymmetrically related chains of hydrogen-bonded molecules oriented along the *a* axis. The chains are also centrosymmetric by themselves as a consequence of the proton disorder [Fig. 3(*a*)].

There is one void left inside the unit cell of the crystal structure of **2** (van der Waals radii from Vainshtein *et al.*[23]) located at the special position (0,1/2,1/2). The total packing coefficient [$Ck = (V_{\mathbf{molecules}})$/unit cell volume] is 0.68.

Table 3 Selected geometrical parameters for compound **2** and hydrogen bond interactions for **2**, **3** and pyrazole (Å, °). Cent(*i*) stands for the geometric centroid of the pyrazole rings.

Molecule	*i* = 1	*i* = 2	Molecule	*i* = 1	*i* = 2
N(*i*01)–N(*i*02)	1.362(3)	1.350(3)	C(*i*05)–C(*i*06)	1.514(3)	1.506(3)
N(*i*01)–C(*i*05)	1.340(3)	1.345(2)	C(*i*06)–C(*i*07)	1.533(3)	1.537(3)
N(*i*02)–C(*i*03)	1.331(3)	1.335(3)	C(*i*06)–C(*i*11)	1.539(3)	1.552(3)
C(*i*03)–C(*i*04)	1.390(3)	1.386(3)	C(*i*06)–C(*i*12)	1.538(4)	1.542(3)
C(*i*04)–C(*i*05)	1.390(3)	1.394(4)			
N(*i*02)–N(*i*01)–C(*i*05)	109.2(2)	109.6(2)	C(*i*04)–C(*i*05)–C(*i*06)	131.9(2)	131.5(2)
N(*i*01)–N(*i*02)–C(*i*03)	107.8(2)	107.9(2)	N(*i*01)–C(*i*05)–C(*i*06)	120.0(2)	120.9(2)
N(*i*02)–C(*i*03)–C(*i*04)	109.5(2)	109.4(2)	C(*i*05)–C(*i*06)–C(*i*12)	109.7(2)	110.5(2)
C(*i*03)–C(*i*04)–C(*i*05)	105.3(2)	105.5(2)	C(*i*05)–C(*i*06)–C(*i*11)	110.0(2)	109.7(2)
N(*i*01)–C(*i*05)–C(*i*04)	108.1(2)	107.6(2)	C(*i*05)–C(*i*06)–C(*i*07)	111.1(2)	111.5(2)
N(*i*01)–C(*i*05)–C(*i*06)–C(*i*07)	170.3(2)	164.8(2)			
N(*i*01)–C(*i*05)–C(*i*06)–C(*i*11)	−70.2(3)	−76.2(3)			
N(*i*01)–C(*i*05)–C(*i*06)–C(*i*12)	50.0(3)	43.9(3)			

Hydrogen bond interactions	X–H	Y ··· H	X ··· Y	X–H ··· Y
Compound **2**				
N(101)–H(101) ··· N(201)	0.97(9)	1.86(9)	2.821(3)	174(8)
N(201)–H(201) ··· N(101)	0.82(9)	2.02(8)	2.821(3)	163(8)
N(102)–H(102) ··· N(102)(1−*x*, 1−*y*, −*z*)	0.89(8)	2.10(8)	2.989(3)	175(7)
N(202)–H(202) ··· N(202)(−*x*, 1−*y*, −*z*)	0.89(6)	2.13(6)	3.029(3)	176(7)
C(103)–H(103) ··· Cent(2)(1−*x*, 1−*y*, −*z*)	0.99(4)	2.56(4)	3.461(3)	151(3)
C(203)–H(203) ··· Cent(1)(−*x*, 1−*y*, −*z*)	0.99(4)	2.55(4)	3.467(3)	154(3)
Pyrazole				
N(101)–H(101) ··· N(202)	1.04(1)	1.90(1)	2.914(10)	164(1)
N(201)–H(201) ··· N(102)(*x*, 3/2 − *y*, −1/2 + *z*)	1.01(1)	1.89(1)	2.902(9)	177(1)
C(103)–H(103) ··· Cent(1)(*x*, 3/2 − *y*, 1/2 + *z*)	1.07(2)	2.64(2)	3.688(6)	165(1)
C(205)–H(205) ··· Cent(2)(*x*, 3/2 − *y*, −1/2 + *z*)	1.10(2)	2.55(2)	3.554(6)	151(1)
Compound **3**				
N(101)–H(101) ··· N(202)	0.87(6)	1.98(6)	2.856(5)	159(6)
N(201)–H(201) ··· N(302)	0.88(8)	2.17(8)	3.023(5)	162(7)
N(301)–H(301) ··· N(402)	0.84(5)	2.01(5)	2.854(5)	154(5)
N(401)–H(401) ··· N(102)(*x*, *y*, *z* + 1)	0.79(8)	2.39(8)	3.133(5)	160(8)
C(103)–H(103) ··· Cent(3)(*x*, *y*, *z* − 1)	0.98(5)	2.77(5)	3.612(5)	144(3)
C(205)–H(205) ··· Cent(4)	0.98(7)	2.95(8)	3.745(6)	139(6)
C(303)–H(303) ··· Cent(1)	0.98(6)	2.78(6)	3.672(5)	151(4)
C(405)–H(405) ··· Cent(2)(*x*, *y*, *z* + 1)	0.95(7)	2.94(7)	3.733(6)	142(5)

4-(1-Adamantyl)pyrazole 3

We have already published the crystal structure as well as the room temperature ^{13}C chemical shifts of this compound in the solid state:[13] there are four independent molecules in the asymmetric unit cell which are linked by hydrogen bonds forming a helix ('catemer') with two of the four adamantyl groups disordered in two orientations with respect to the pyrazole ring [see Fig. 2(*d*)]. Large thermal ellipsoids were found for both nitrogen atoms N1 and N2 indicating some disorder involving the NH protons. In the ^{13}C CP MAS NMR spectrum, recorded at room temperature, we reported broad signals for the C3 and C5 carbon atoms which we interpreted as indicative of NH proton disorder, corroborating the X-ray results. Moreover, there is a splitting of the C5 signal arising from the existence of two main types of molecule in the unit cell.

In the present study we measured the ^{15}N CP MAS NMR spectra of $^{15}N_2$-labelled **3** as a function of temperature. The superimposed experimental and calculated spectra are shown in Fig. 4. At room temperature (300 K), there is again a large splitting of the =N– signal at 251.7 and 242.7 ppm, whereas the proton-bearing nitrogen atoms show a single line at 166.5 ppm. Since the crystal structure determined by X-ray crystallography is known,[13] one could explain the CP MAS NMR results in terms of two non-protonated nitrogen atoms experiencing the effect of two adamantyl groups in different crystallographic situations, one of the adamantyl groups presenting 'conformational' disorder about the adamantyl–pyrazole CC bond, in contrast to the second adamantyl group which shows a definite conformation, as indicated by X-ray crystallography. As in compound **2**, this influence is less pronounced in the case of the protonated nitrogen atoms.[5] Furthermore, since both =N– signals appear to have nearly the same line-width which does not change at low temperature (227 K), one could conclude that the conformational disorder of the adamantyl groups must be static so that the nitrogen atoms experience the effect of an average conformation. If the conformational disorder were dynamic, at low temperature a distribution of different adamantyl group conformations should be reflected in a larger line-width for one of the two =N– signals, which is not the case.[5]

As the temperature is raised, a slight broadening of all signals is observed, indicating a very slow quadruple proton transfer between nitrogen sites. Note that all three signals broaden simultaneously and that there is no sign of exchange between the two =N– signals. Provided that there is no change in the crystal structure at higher temperatures, we can assume that the proton transfer takes place between two chemically exchanging systems with different conformations of the adamantyl group. The first one involves pyrazole molecules bearing adamantyl groups which show a static conformational disorder. The second one includes pyrazole molecules bearing adamantyl groups with a

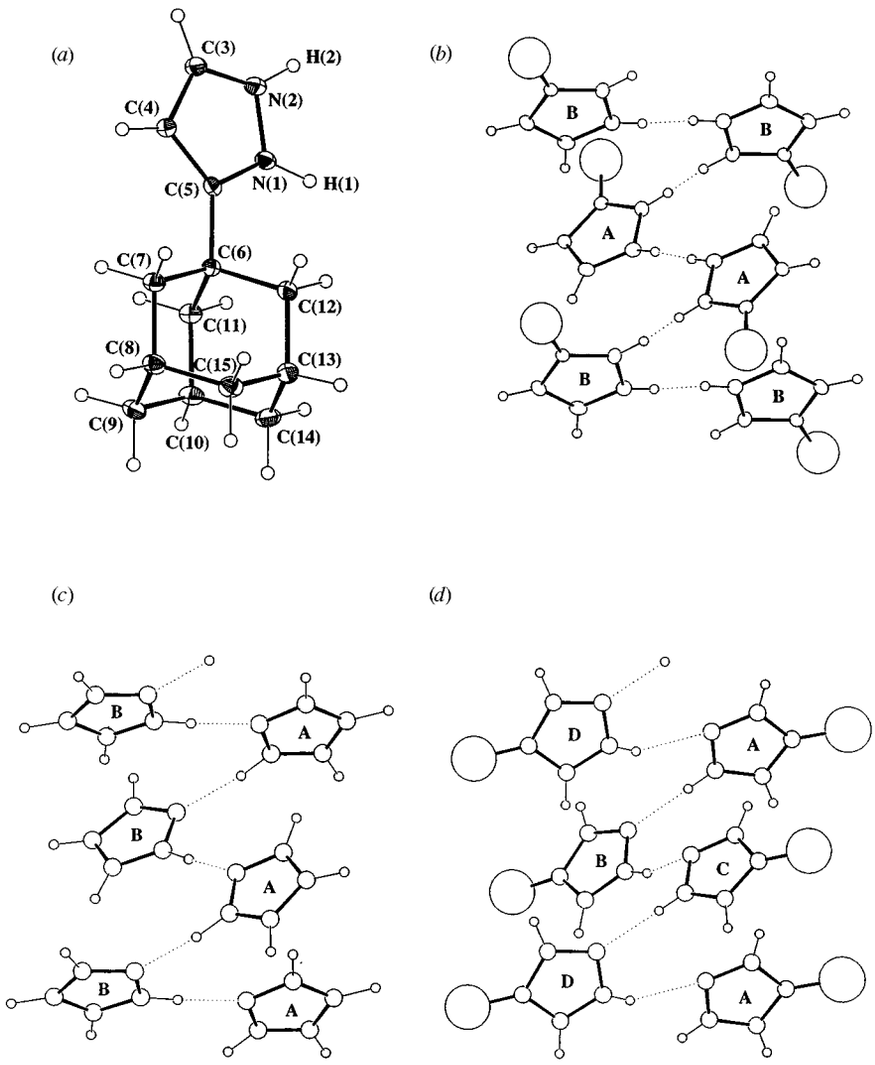

Fig. 2 (*a*) ORTEP[31] view of one crystallographically independent molecule of compound **2** showing the numbering scheme. The 1:1 hydrogen disorder is plotted for both tautomeric positions [**2a**, N(1)–H(1); **2b**, N(2)–H(2)]. Ellipsoids are drawn at 30% probability level. (*b*), (*c*), (*d*) Extended views of the hydrogen bonded chains of molecules in the same orientation for compounds **2**, pyrazole and **3**, respectively. Dotted lines indicate hydrogen bonds and the bulky substituents represent the 1-adamantyl group. Crystallographically independent molecules have been labelled to clarify the hydrogen bond interactions shown in Table 3.

Table 4 Rate constants obtained by line-shape analysis of the proton transfer in 4-(1-adamantyl)pyrazole **3** and 3,5-dimethyl-4-(1-adamantyl)pyrazole **4**

Compound **3**		Compound **4**	
T/K	k_{12}/s^{-1}	T/K	k_{12}/s^{-1}
227	<10	328	500
300	<10	338	820
353	30	348	1210
396	130	357	1700
413	220	368	2430

given conformation. If the two systems could interconvert through rotation of the adamantyl groups, both =N– signals should coalesce into a single line reflecting an average conformation of the adamantyl groups,[5] but this is again not the case. Since the pyrazole molecule is symmetrically substituted the spectra were calculated assuming two two-site systems with different =N– chemical shifts but with identical N–H chemical shifts, and an equilibrium constant of $K_{12} = 1$. Although the rate constants k_{12} were determined in the slow exchange regime, where line-shape analysis is not very accurate, and only for three points, they can be used at least as estimated values for the proton transfer. They are assembled in Table 4. The reaction rates obtained can be expressed by the corresponding Arrhenius equation (1).

$$k_{12} \approx 10^{7.4} \exp(-40.1 \text{ kJ mol}^{-1}/RT) \quad (1)$$

In view of the crystal structure of this compound where a helix is present, it is very unlikely that a proton transfer takes place between the very large number of molecules of the 'catemer.' There is no such example reported in the literature; more probably, one can assume that a change in the crystal structure must take place at higher temperatures allowing the proton transfer, which is, by the way, very slow as compared to other pyrazole derivatives. However, since a crystal structure analysis at higher temperature could not be performed on the diffractometers at our disposal (highest temperature: 340 K) these conclusions are only tentative.

3,5-Dimethyl-4-(1-adamantyl)pyrazole 4

Attempts were made to determine the crystal structure of this compound. Although apparently good crystals were obtained, the structure cannot be solved. It is probable that this compound is a plastic crystal like adamantane itself.[11,12]

Fig. 5 shows the superimposed experimental and calculated ^{15}N CP MAS NMR spectra of **4** at different temperatures. At low temperature (230 K), this time, only two signals are

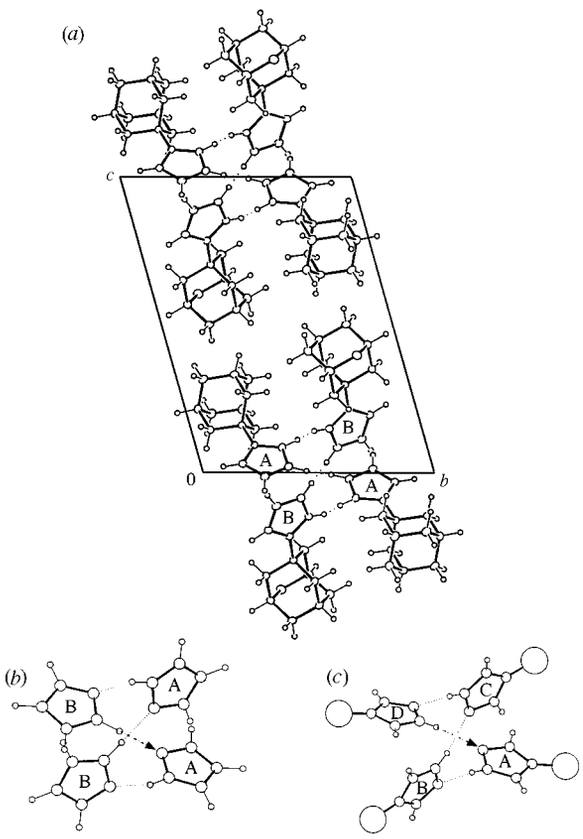

Fig. 3 (*a*) Crystal structure as projected down the *a* axis for compound **2**. (*b*) Parallel view of one chain of hydrogen-bonded molecules for the parent compound. The view is the equivalent to the projection along the crystallographic *c* axis. Dotted lines indicate hydrogen bonds, with the arrow representing the connection with the molecule translated by the length of the unit cell axis. (*c*) Same as (*b*) for compound **3**. The bulky substituents represent the 1-adamantyl group. [The dotted arrow has been omitted in (*a*) for clarity.]

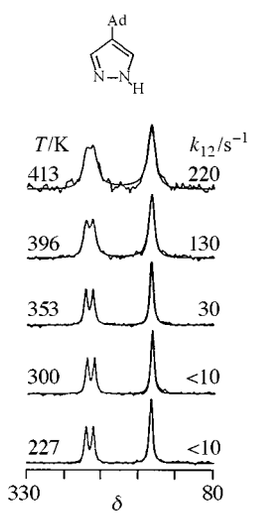

Fig. 4 9.12 MHz superimposed experimental and calculated ^{15}N CP MAS NMR spectra of **3** recorded at different temperatures: sweep width 7 kHz, CP times of 4–6 ms, average number of scans 1200, line broadening 20, k_{12} is the forward constant

observed arising from the protonated (166.6 ppm) and non-protonated nitrogen atoms (240.5 ppm). We note that both lines exhibit the same intensity as well as a clearly larger line-width as compared to the other compounds studied in this work. This could arise either from a distribution of pyrazole molecules with the adamantyl group in different fixed time-independent conformations, or from a distribution of different pyrazole associates such as dimers, trimers, tetramers or even larger ones

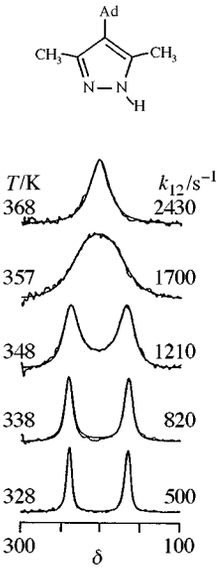

Fig. 5 9.12 MHz superimposed experimental and calculated ^{15}N VT CP MAS NMR spectra of **4**: sweep width 7 kHz, CP times of 2–8 ms, average number of scans 600, line broadening 20, k_{12} is the forward rate constant

with the adamantyl group showing dynamic disorder, *i.e.* time-dependent conformations. This second explanation seems to us more plausible in view of the plastic properties expected for crystals of compound **4** and of the large temperature range of coalescence of nearly 60 °C as compared to other pyrazoles where it is only about 30 °C. When the temperature is raised, the two lines broaden, coalesce and, at high temperature, give rise to a single central line indicating a degenerate proton exchange between two equally populated states, *i.e.* an equilibrium constant for the tautomerism of $K_{12} = 1$.[3] The spectra were again calculated assuming two two-site systems with different =N– and N–H chemical shifts, the results being very satisfactory (see Fig. 5). However, the rate constants obtained (see Table 4) must be regarded as average values for the proton transfer processes in the different pyrazole associates present in the crystal. Eqn. (2) can be obtained from the corresponding Arrhenius plot.

$$k_{12} \approx 10^{9.0} \exp(-39.5 \text{ kJ mol}^{-1}/RT) \qquad (2)$$

3,5-Di(1-adamantyl)pyrazole 5

Due to the presence of two 1-adamantyl substituents, this compound might be a plastic crystal like compound **4**. In the ^{13}C CP MAS NMR spectrum recorded at room temperature broad signals are observed for the C3 and C5 carbon atoms at 144.4 and 134.3 ppm, respectively (see Table 1) indicative of dynamic proton disorder in the nitrogen sites. The ^{15}N CP MAS NMR spectra for the labelled compound confirm this assumption. The superimposed experimental and calculated spectra are depicted in Fig. 6. As expected, there are two lines at low temperature corresponding to the =N– (241 ppm) and N–H (159.6 ppm) nitrogen atoms. The different adamantyl conformations are again reflected in a larger line-width of the =N– signal as compared to the N–H one. As the temperature is raised the lines broaden, sharpen again and move inwards; this is characteristic of a non-degenerate proton transfer between unequally populated states. This is not surprising since the conformational disorder of the adamantyl groups can lead to an asymmetric system, though the pyrazole ring is symmetrically substituted, just as in the case of compound **1**.[5] From the line-splitting at low temperature, where the transfer is frozen, and from the splittings at high temperature, the temperature-dependent equilibrium constants can be obtained.[5] A van't Hoff analysis of these data yields at room temperature (298 K) an equilibrium constant of $K_{12} = 0.287$ corresponding to 78% of the major tautomer. Moreover, a reaction enthalpy of $\Delta H_{12} = 3.9$ kJ mol^{-1}

and a reaction entropy of $\Delta S_{12} = 4.3$ J K^{-1} mol^{-1} were obtained, which are small values indicating a small asymmetry of the system. This is confirmed at high temperature where a small line-splitting is observed in the spectrum recorded at 373 K. The value of $K_{12} = 0.508$ found at this temperature corresponds to 66% of the major tautomer, not far from the value of 50% present in a degenerate process. This could again be a sign that the small asymmetry is caused by the conformational disorder of the adamantyl groups.

Due to the larger line-width of the =N− signal, the spectra were calculated assuming two two-site systems with different =N− and the same N−H chemical shifts, as in the case of the preceding pyrazoles. The rate constants k_{12} obtained (see Table 5) were fitted to the Arrhenius equation (3).

$$k_{12} = k_{21}/K_{12} = ca.\ 10^{9.6} \exp(-39.0 \text{ kJ mol}^{-1}/RT) \quad (3)$$

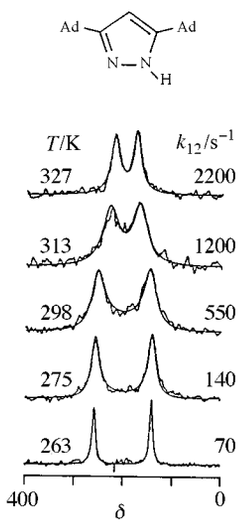

Fig. 6 9.12 MHz superimposed experimental and calculated ^{15}N VT CP MAS NMR spectra of **5**: sweep width 7 kHz, CP times of 2–8 ms, average number of scans 800, line broadening 20, k_{12} is the forward rate constant

Table 5 Temperature dependence of the equilibrium constant K_{12} obtained by linear regression of the experimental data (x_1 is the mole fraction of the predominant tautomer) and forward rate constants k_{12} obtained by line-shape analysis of the proton transfer in 3,5-di-(1-adamantyl)pyrazole **5**

T/K	K_{12}	x_1	k_{12}/s^{-1}
245	0.155	0.86	<10
252	0.171	0.85	<10
263	0.197	0.84	70
275	0.226	0.82	140
298	0.287	0.78	550
313	0.329	0.75	1200
327	0.369	0.73	2200
373	0.508	0.66	>5000

Conclusions

Regarding molecular dynamics, the four adamantylpyrazoles show four different types of behaviour. In spite of the fact that only two X-ray structures were solved (compounds **2** and **3**), the use of VT ^{15}N CP MAS NMR allows some tentative and some definitive conclusions to be drawn. In Table 6 we have summarized the most relevant information. Compound **2** (the 1:1 mixture of **2a** and **2b** according to X-ray crystallography) is a 'catemer' and as in most catemers there is no proton transfer.[4] In this sense, the use of K_{12} in Table 6 is not entirely correct since there is no 'equilibrium' between the two tautomers, only a 1:1 mixture. Compound **3** may be an exception and be the only 'catemer' showing proton transfer. A possible explanation for this exceptional behaviour is that the proton transfer is coupled with a rotation (**X**) about the C4−Ad1 bond.

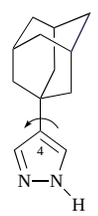

X

Compounds **4** and **5** should be cyclic structures, dimers or trimers (tetramers are less common)[24] but the activation energies of *ca.* 39 kJ mol^{-1} are relatively low compared with those of 3,5-dimethylpyrazole (trimer, $E_a = 50.5$ kJ mol^{-1}) and 3,5-di-*tert*-butylpyrazole **1** (dimer, $E_a = 56.6$ kJ mol^{-1}).[24] Probably, the quasi-spherical shape of the 1-adamantyl substituent and its crystal plasticity play a role in lowering these barriers.

Experimental

Materials

[$^{15}N_2$]-Derivatives were prepared starting from [$^{15}N_2$]hydrazine sulfate (from Chemotrade, Leipzig, FRG). [$^{15}N_2$]Pyrazole and 3,5-dimethylpyrazole were synthesized according to published procedures.[2,25] 4-(1-Adamantyl)- **3** and 3,5-dimethyl-4-(1-adamantyl)[$^{15}N_2$]pyrazole **4** were then prepared by *C*-adamantylation of the corresponding $^{15}N_2$-labelled pyrazoles using 1-bromoadamatane.[13] 3(5)-(1-Adamantyl)pyrazole **2** and 3,5-di(1-adamantyl)pyrazole **5** were also obtained by *C*-adamantylation of pyrazole, changing the regioselectivity of the adamantylation in a microwave oven; attention should be paid to the reaction time that should be 5 min at 600 W instead of 3 min as stated in ref. 26. *C*-Adamantylation of pyrazole with 1-bromoadamantane carried out at 13 kbar and 70 °C for 24 h failed however; starting materials were recovered unchanged.[27] Labelled pyrazoles **3**, **4** and **5** have melting points identical with those of the corresponding unlabelled compounds;[13,26] they have been identified by mass spectrometry.

Table 6 Summary of the structural conclusions regarding adamantylpyrazoles **2**–**5**

	2a **2b**	**3**	**4**	**5**
X-Ray crystallography	Catemer NH disorder: **2a**/**2b** 1:1	Catemer NH disorder Ad disorder	Unknown	Unknown
NMR:				
Adamantyl groups	Ordered	Some ordered some disordered	Ordered	Disordered
Pyrazole NH tautomerism	$K_{12} = 1$ No proton transfer	$K_{12} = 1$ Proton transfer $E_a = 40.1$ kJ mol^{-1} [eqn. (1)]	$K_{12} = 1$ Proton transfer $E_a = 39.5$ kJ mol^{-1} [eqn. (2)]	$K_{12} \neq 1$ Proton transfer $E_a = 39.0$ kJ mol^{-1} [eqn. (3)]

Table 7 Crystal parameters at 150 K for compound **2**

Crystal data	
Formula	$C_{13}H_{18}N_2$
Crystal habit	Colourless, plate
Crystal size (mm)	0.05 × 0.13 × 0.40
Symmetry	Triclinic, $P\bar{1}$
Unit cell determination:	Least-squares fit from 69 reflexions (θ < 45°)
Unit cell dimensions/Å, °	a = 6.8576(4)
	b = 11.4443(13)
	c = 14.7994(20)
	104.895(11), 91.093(5), 102.726(5)
V/Å^3, Z	1091.3(2), 4
D_c/g cm^{-3}, M, F(000)	1.231, 202.30, 440
μ/cm^{-1}	5.60
Experimental data	
Technique	Four-circle diffractometer: Philips PW1100, Bisecting geometry. Graphite-oriented monochromator. ω–2θ scans. Detector apertures 1 × 1°. 1 min/reflex. Radiation: Cu-Kα Scan width: 1.5°; θ_{max} = 65°
Number of reflexions:	
Independent	3694
Observed	2931 [2σ(I)]
Standard reflexions:	2 reflexions every 90 min. No variation
Max.–min. Transmission factors	1.000–0.917
Solution and refinement	
Solution	Direct methods: Sir92
Refinement:	
Least-squares on F_o	Full matrix
Parameters:	
Number of variables	385[a]
Degrees of freedom	2546
Ratio of freedom	7.6
Final shift/error	0.07
H atoms	From difference synthesis
Secondary extinction factor (×10^4)	0.153(6)
Weighting scheme	Empirical so as to give no trends in $\langle\omega\Delta^2F\rangle$ *vs.* $\langle\|F_{obs}\|\rangle$ and $\langle\sin\theta/\lambda\rangle$
Max. anisotropic displacement parameters/Å^2	U_{11}[C(214)] = 0.039(1)
Final ΔF peaks/e Å^{-3}	±0.29
Final R and R_w	0.048, 0.054

[a] See Experimental.

1-Methyl-3-(1-adamantyl)pyrazole 6 and 1-methyl-5-(1-adamantyl)pyrazole 7

A mixture of 0.1 g (0.49 mmol) of 3(5)-(1-adamantyl)pyrazole **2**, 0.2 g (1.47 mmol) of anhydrous K_2CO_3, 0.06 g (0.98 mmol) of KOH and 0.04 ml (0.59 mmol) of CH_3I in 3 ml of anhydrous acetone was heated under reflux for 4 h. After cooling, the solvent and excess of CH_3I were evaporated under reduced pressure and the *N*-methylpyrazoles **6** and **7** were separated by column chromatography using as eluent dichloromethane–ethanol (99:1) and isolated as oils. The same procedure was followed to obtain 1-methyl-3-(1-adamantyl)[$^{15}N_2$]pyrazole **6** and 1-methyl-5-(1-adamantyl)[$^{15}N_2$]pyrazole **7**. Compound **6**: yield (isolated product) 70%; R_f (dichloromethane–ethanol, 99:1) 0.64; ^{1}H NMR ($CDCl_3$) δ 1.76 [6H, t, ^3J(H-γ) 2.9, H-δ Ad], 1.94 (3H, d, H-β Ad), 2.04 (3H, br s, H-γ Ad), 3.85 [3H, dd, $^2J(^{15}N\text{-}1) = {}^3J(^{15}N\text{-}2) = 1.8$, 1-Me], 6.05 [1H, ddd, $^3J(^{15}N\text{-}2)$ 0.9, ^3J(H-5) 2.2, $^3J(^{15}N\text{-}1)$ 6.0, H-4], 7.23 [1H, dd, $^2J(^{15}N\text{-}1)$ 4.5, H-5]; ^{13}C NMR ($CDCl_3$) δ 28.6 (^1J 133.1, C-γ Ad), 33.8 [$^2J(^{15}N\text{-}2)$ 6.0, $^3J(^{15}N\text{-}1)$ 2.8, C-α Ad], 36.8 (^1J = 258.3, C-δ Ad), 38.6 [^1J 139.1, $^1J(^{15}N\text{-}1)$ 14.4, $^2J(^{15}N\text{-}2)$ 6.1, Me-1], 42.8 (^1J 255.8, C-β Ad), 101.0 [^1J 173.7, ^2J 8.6, $^2J(^{15}N\text{-}2)$ 5.1, $^2J(^{15}N\text{-}1)$ 1.9, C-4], 129.9 (^1J 183.6, ^2J 8.8, ^3J 2.6, C-5), 162.5 (C-3). Compound **7**: yield (isolated product) 25%; R_f (dichloromethane–ethanol, 99:1) 0.36; ^{1}H NMR ($CDCl_3$) δ 1.77 (6H, br s, H-δ Ad), 2.01 [3H, d, ^3J(H-γ) 2.7, H-β Ad], 2.08 (3H, br s, H-γ Ad), 4.01 [3H, dd, $^2J(^{15}N\text{-}1) = {}^3J(^{15}N\text{-}2) = 2.0$, 1-Me], 5.98 [1H, ddd, $^3J(^{15}N\text{-}2)$ 1.1, ^3J(H-3) 1.95, $^3J(^{15}N\text{-}1)$ 5.6, H-4], 7.33 [1H, ddd, $^2J(^{15}N\text{-}2)$ 12.5, $^3J(^{15}N\text{-}1)$ 8.0, H-3]; ^{13}C NMR ($CDCl_3$) δ 28.3 (^1J 133.1, C-γ Ad), 33.4 (C-α Ad), 36.5 (^1J 255.1, C-δ Ad), 39.8 [^1J 139.3, $^1J(^{15}N\text{-}1)$ 13.8, $^2J(^{15}N\text{-}2)$ 6.7, Me-1], 40.8 (^1J 254.0, C-β Ad), 103.4 (^1J 174.8, C-4), 137.4 (^1J 183.1, ^2J 5.2, C-3), 151.1 (C-5).

NMR spectroscopy

The ^{1}H, ^{13}C and ^{15}N NMR spectra in solution were recorded on a Bruker AC200 instrument working at 200.16 (^{1}H), 50.32 (^{13}C) and 20.29 MHz (^{15}N) using standard conditions. The ^{15}N NMR chemical shifts in $CDCl_3$ solution were measured for **2** (−156.7 and −124.5 ppm), **3** (−138.0 ppm), **4** (−141.6 ppm), **5** (−147.0 ppm), **6** (−187.9, NMe and −83.9, −N=) and **7** (−185.4, NMe and −74.8, −N=) [1-methyl-4-(1-adamantyl)pyrazole: −184.9, NMe and −78.6, −N=]. These chemical shifts are referred to external CH_3NO_2. To compare these shifts with those determined in the solid state (reference solid $^{15}NH_4Cl$) a 346.4 ppm correction must be applied [δ^{15}N(solid) = 346.4 + δ^{15}N(solution)] (we have previously used 355.3 ppm).[15] J Values are given in Hz.

CP MAS NMR spectroscopy

^{13}C CP MAS NMR spectra were obtained at room temperature on a Bruker AC200 spectrometer (UNED). For this purpose a 7 mm Bruker DAB 7 probehead was used that achieves rotation frequencies of about 3–4.5 kHz. The standard CP pulse sequence was applied[28] with a 7 s ^{1}H-90° pulse width, 2–5 ms contact pulses, 5 s repetition time and a spectra width of 20 kHz. ^{13}C Chemical shifts are given with respect to the spectrometer reference frequency which was callibrated by the glycine signal at 176.1 ppm.

The ^{15}N CP MAS NMR spectra were recorded on a Bruker CXP-100 spectrometer (F. U. Berlin) working at 9.12 MHz for ^{15}N and 90.02 MHz for protons. The spectrometer is equipped with a 7 mm CP MAS probehead from Doty Scientific, USA. The spinning speeds were of the order of 2–3 kHz. A Bruker B-VT-1000 temperature unit was used to control the temperature of the bearing nitrogen gas stream and a home-built heat exchanger was employed in order to achieve low temperatures. The sample temperatures were determined by using a 2 × 3 mm platinum resistance thermometer, PT-100, from Degussa. It was placed approximately 3 mm from the coil. No interferences during NMR signal acquisition were observed. The standard CP pulse sequence was again performed.[28] General recording parameters: quadrature detection, 5.5 s ^{1}H-90° pulse width, 2–8 ms CP times, 4 s recycle delay, spectral width of 7 kHz, line broadening of 20 Hz. All ^{15}N chemical shifts are related to external solid $^{15}NH_4Cl$ and given with an error of ±0.3 ppm.

X-Ray analysis

Table 7 summarizes the main details of data collection and processing. Data were collected at 150 K using an Oxford Cryostream device[29] and the stated temperature was measured continuously during data collection. The structure was solved by direct methods, Sir92,[30] and refined on F_{obs} by least-squares procedures. The hydrogen atoms, located by Fourier difference synthesis, were refined isotropically, but their thermal parameters were fixed in the last weighted cycles of refinement. Most of the calculations were performed on a DEC3000-300X workstation using the Xtal3.4 System.[31] The atomic scattering factors were taken from the *International Tables for X-Ray Crystallography*, vol. IV.§,[32]

Acknowledgements

Thanks are given on the EU for the TMR network 'Localization and Transfer of Hydrogen' (No. CHRX CT 940582). Financial support was provided by the Spanish DGICYT (Project nos. PB93-0197-C-02 and PB93-0125). We thank Professor Lutz F. Tietze (Institut für Organische Chemie, Göttingen) who carried out the high pressure experiments and to the referees for considerably improving our manuscript.

§ Atomic coordinates, hydrogen atom parameters and thermal parameters for the non-hydrogen atoms have been deposited at the Cambridge Crystallographic Data Centre. See 'Instructions for Authors', *J. Chem. Soc., Perkin Trans. 2*, 1997, Issue 1. Any request to the CCDC for the material should quote the full literature citation and reference number 188/82.

References

1 A. Baldy, J. Elguero, R. Faure, M. Pierrot and E. J. Vincent, *J. Am. Chem. Soc.*, 1985, **107**, 5290.
2 J. A. S. Smith, B. Wehrle, F. Aguilar-Parrilla, H.-H. Limbach, C. Foces-Foces, F. H. Cano, J. Elguero, A. Baldy, M. Pierrot, M. M. T. Khurshid and J. B. Larcombe-McDouall, *J. Am. Chem. Soc.*, 1989, **111**, 7304.
3 F. Aguilar-Parrilla, G. Scherer, H.-H. Limbach, C. Foces-Foces, F. H. Cano, J. A. S. Smith, C. Toiron and J. Elguero, *J. Am. Chem. Soc.*, 1992, **114**, 9657.
4 J. Elguero, F. H. Cano, C. Foces-Foces, A. L. Llamas-Saiz, H.-H. Limbach, F. Aguilar-Parrilla, R. M. Claramunt and C. López, *J. Heterocycl. Chem.*, 1994, **31**, 695.
5 F. Aguilar-Parrilla, H.-H. Limbach, C. Foces-Foces, F. H. Cano, N. Jagerovic and J. Elguero, *J. Org. Chem.*, 1995, **60**, 1965.
6 J. Elguero, N. Jagerovic, C. Foces-Foces, F. H. Cano, M. V. Roux, F. Aguilar-Parrilla and H.-H. Limbach, *J. Heterocycl. Chem.*, 1995, **32**, 451.
7 H.-H. Limbach, G. Scherer, L. Meschede, F. Aguilar-Parrilla, B. Wehrle, J. Braun, C. G. Hoelger, H. Benedict, G. Buntkowsky, W. P. Fehlhammer, J. Elguero, J. A. S. Smith and B. Chaudret, *Ultrafast Reaction Dynamics and Solvent Effects, Experimental and Theoretical Aspects*, ed. Y. Gaudel and P. J. Rossky, American Institute of Physics, 1993, pp. 225–239.
8 J.-L. G. de Paz, J. Elguero, C. Foces-Foces, A. L. Llamas-Saiz, F. Aguilar-Parrilla, O. Klein and H.-H. Limbach, *J. Chem. Soc., Perkin Trans. 2*, 1997, 101.
9 F. Aguilar-Parrilla, H.-H. Limbach, J. Elguero and J. A. S. Smith, unpublished results.
10 F. G. Riddell, S. Arumugam, K. D. M. Harris, M. Rogerson and J. H. Strange, *J. Am. Chem. Soc.*, 1993, **115**, 1881.
11 M. Foulon, T. Belgrand, C. Gors and M. More, *Acta Crystallogr., Sect. B*, 1989, **45**, 404.
12 Y. Huang, D. F. R. Gilson, I. S. Butler and F. Morin, *J. Phys. Chem.*, 1991, **95**, 2151.
13 P. Cabildo, R. M. Claramunt, I. Forfar, C. Foces-Foces, A. L. Llamas-Saiz and J. Elguero, *Heterocycles*, 1994, **37**, 1623.
14 F. Aguilar-Parrilla, R. M. Claramunt, C. López, D. Sanz, H.-H. Limbach and J. Elguero, *J. Phys. Chem.*, 1994, **98**, 8752.
15 F. Aguilar-Parrilla, F. Männle, H.-H. Limbach, N. Jagerovic and J. Elguero, *Magn. Reson. Chem.*, 1994, **32**, 699.
16 F. Aguilar-Parrilla, C. Cativiela, M. D. Díaz de Villegas, J. Elguero, C. Foces-Foces, J. I. G. Laureiro, F. H. Cano, H.-H. Limbach, J. A. S. Smith and C. Toiron, *J. Chem. Soc., Perkin Trans. 2*, 1992, 1737.
17 R. Notario, M. Herreros, A. El Hammadi, H. Homan, J. L. M. Abboud, I. Forfar, R. M. Claramunt and J. Elguero, *J. Phys. Org. Chem.*, 1994, **7**, 657.
18 A. El Hammadi, M. El Mouhtadi, R. Notario, J. L. M. Abboud and J. Elguero, *J. Chem. Res.*, 1995, (*S*) 172; (*M*) 1080.
19 F. K. Larsen, M. S. Lehmann, I. Søtofte and S. E. Rasmussen, *Acta Chem. Scand.*, 1970, **24**, 3248.
20 A. L. Llamas-Saiz, C. Foces-Foces and J. Elguero, *J. Mol. Struct.*, 1994, **319**, 231.
21 A. Domenicano and P. Murray-Rust, *Tetrahedron Lett.*, 1979, **24**, 2283 and references therein.
22 D. Cremer and J. A. Pople, *J. Am. Chem. Soc.*, 1975, **97**, 1354.
23 B. K. Vainshtein, V. M. Fridkin and V. L. Indenbom, *Modern Crystallography II*, Springer-Verlag, Berlin, 1982, p. 87.
24 F. Aguilar-Parrilla, O. Klein, H.-H. Limbach, C. Fernández-Castaño, C. Foces-Foces, N. Jagerovic and J. Elguero, unpublished results.
25 J. Berthou, J. Elguero and C. Rérat, *Acta Crystallogr., Sect. B*, 1970, **26**, 1881.
26 I. Forfar, P. Cabildo, R. M. Claramunt and J. Elguero, *Chem. Lett.*, 1994, 2079.
27 L. F. Tietze, personal communication.
28 C. A. Fyfe, *Solid State NMR for Chemists*, C. F. C. Press, Guelph, Ontario, 1983.
29 J. Cosier and A. M. Glazer, *J. Appl. Crystallogr.*, 1986, **19**, 105.
30 Sir92: A. Altomare, M. C. Burla, M. Camalli, G. Cascarano, C. Giacovazzo, A. Guagliardi and G. Polidori, *J. Appl. Crystallogr.*, 1994, 435.
31 Xtal3.4: S. R. Hall, C. S. D. King and J. M. Stewart, 1995, University of Western Australia, Lamb, Perth.
32 *International Tables for X-Ray Crystallography*, Kynoch Press, Birmingham, 1974, vol. IV.

Paper 6/07436G
Received 1*st November* 1996
Accepted 29*th April* 1997